Original article

Stemflow and throughfall determination in a resprouted Mediterranean holm-oak forest

Juan Bellot*, Antonio Escarre

Departamento Ecologia, Universidad de Alicante, Apdo 99, Alicante, Spain

Abstract – Stemflow, throughfall and precipitation data were collected for 30 consecutive months in a holm-oak forest dominated by *Quercus ilex*, *Arbutus unedo* and *Phyllirea media*. These flux data were obtained from 50 randomly distributed no-roving throughfall collectors and 20 stemflow measuring devices (ten on *Q. ilex* and five on each of the other species). The stemflow was highly influenced by tree size and amount of rainfall, showing a significant correlation for each tree. Throughfall results showed a high spatial variability for each storm, with a significant independence of collectors. At forest scale, stemflow and throughfall represented 12.1 and 75 % of precipitation, respectively, and interception was estimated as 12.9 % of precipitation. Partitioning of rainfall between stemflow and throughfall created a high spatial heterogeneity of water distribution under the canopy. Stemflow increased more than 30 times the mean amount of water received per unit soil area around tree trunks. Finally, the effect of a change in the amount of precipitation according to a regional scenario was analyzed. It was shown that the increase in high rainfall events rather than small events increased the stemflow percentage. (©Inra /Elsevier, Paris.)

holm oak / stemflow / throughfall / spatial heterogeneity / interception

Résumé – Évaluation de l'écoulement et de l'égouttement dans une forêt méditerranéenne de Chêne vert. L'écoulement, l'égouttement et l'interception des précipitations ont été mesurés pendant 30 mois consécutifs dans la chênaie de Prades (Espagne), dominée par *Quercus ilex*, *Arbutus unedo* et *Phyllirea media*. Cinquante pluviomètres ont été placés de façon aléatoire dans la forêt, et 20 colliers de mesure d'écoulement le long des troncs ont été installés sur les trois espèces dominantes. L'écoulement le long des troncs est fortement influencé par l'âge des arbres (diamètre des troncs) et par la précipitation incidente, présentant une bonne corrélation avec ces variables. L'égouttement montre une grande variabilité pour chaque averse, et une indépendance statistique significative d'un collecteur à l'autre. À l'échelle forêt, on conclut que l'écoulement représente une importante entrée d'eau dans le sol (12,1 % des précipitations), l'égouttement présente un niveau similaire aux autres forêts (75 %), et l'interception par le couvert atteint 12.9 % des précipitations. La répartition de la pluie entre écoulement et égouttement induit une forte variabilité spatiale de la distribution de l'eau sur le sol, et cette hétérogénéité augmente avec la densité du couvert. L'écoulement multiplie par 30

* Correspondence and reprints
E-mail: juan.bellot@ua.es

l'apport d'eau par unité de surface autour des troncs. Finalement, l'effet d'un possible changement climatique, avec une augmentation des fortes pluies, a été analysé. Les résultats montrent une augmentation de l'écoulement le long des troncs, et ses effets sur le bilan hydrique au niveau du bassin versant sont discutés. (©Inra /Elsevier, Paris.)

chênaie / écoulement / égouttement / hétérogénéité spatiale / interception

1. INTRODUCTION

From the hydrological point of view, the forest canopy could be considered as a filter layer allowing rainfall water to pass through its gap structure. In this approach, the tree crowns and stems form a funnel which takes water from the filter layer and conveys it down the stems to the soil [6, 30]. The stem density and diameter distribution represent the number and sizes of the funnels of the forest canopy layer, respectively. Both influence the amount of stemflow, the spatial variation in the redistribution of non-intercepted rainfall, as well as the hydrological cycle of forested catchments [11, 43]. The effect is a high spatial and temporal variation in stemflow and throughfall as a consequence of the canopy structure and precipitation conditions. Dripping points, gap and funnel distributions in space, determine the spatial heterogeneity in the input of water to the forest soil.

The role of the canopy in the redistribution of precipitation inputs to the forest soil has been well studied in both temperate and tropical ecosystems ([1, 2, 16, 20, 21, 22, 24, 32, 37, 38, 41], and many other studies). Most of these papers emphasize the importance of throughfall as the major water flow on aboveground vegetated surfaces in the canopy. Stemflow has been neglected or even not measured in many of the hydrological studies carried out in forest ecosystems [23, 27, 33], because it is believed to represent a small percentage of precipitation. However, Aussenac [3] and Herwitz [21] reported high stemflow values in some temperate and tropical forests, respectively, due to the combination of high rainfall intensities and the funnelling effect. Recently,

Hanchi and Rapp [18] have reported the importance of the technique used to determine stemflow in forest stands to obtain precise and reliable results. A method based on the correlation between stemflow volume and the respective tree diameter at breast height (DBH) seems to be the most convenient to calculate the total stemflow for a stand. In arid and semi-arid regions, some studies have found a high concentration of water input close to the stems [17, 31]. In these cases, stemflow could represent an important input of water to be used by the plant, because it is more easily infiltrated through the root macropores [8] unless it reaches the ground surface as a spatially concentrated input exceeding infiltration capacity. This infiltration represents a self-supply of water to the area around the root system [15, 31].

According to the literature reviewed [14, 23, 32, 33], stemflow should constitute a small percentage of precipitation (0–5%), which contrasts with the 12 % measured in the resprouted Mediterranean holm-oak forest of Prades [5]. The difference could be explained by the high tree density and the frequency of intense, large storm events common to the Mediterranean climate. Whereas the first reason is linked to the structural characteristics of the forest, the second may modify the degree of stemflow according to the climatic conditions in this or in other areas. The generalization of this precipitation regime, frequent in semi-arid Mediterranean areas [34], to other forested regions would represent an increase in stemflow and consequently a reduction in superficial runoff and erosion. On this assumption, a climatic scenario such as that proposed by Rambal and Debussche [39],

which predicts a change in the number and distribution of rainfall events – even with minor changes in the total annual rainfall – could affect the forest hydrology through increased stemflow and infiltration [9, 10, 26].

The aim of this paper is to analyze the rainfall partitioning between throughfall, stemflow and interception in a Mediterranean holm-oak forest under a characteristic precipitation regime. As these patterns can be similar to those occurring in other areas if the precipitation regime changes, they can be used to estimate the hydrological consequences of these trends. In particular, this study stresses the role of vegetation in: 1) channelling rainfall water by stemflow and producing the variability of throughfall on the forest soils; 2) redistributing the rainfall through the canopy water pathways; and 3) modifying stemflow and throughfall partitioning due to the effects of changes in the precipitation regime.

2. MATERIALS AND METHODS

2.1. Study area

The study was carried out at Prades experimental station in the province of Tarragona, N.E. Spain. The forest covers the Poblet mountains where there are some gauged instrumented watersheds (41° 13' N, 1° 10' E): the Avic, Teula and Saucar, with catchment areas between 24 and 53 ha, mean slopes from 25.2 to 28.5°, and altitudes ranging from 650 to 1 135 m a.s.l. The geological material is mainly palaeozoic slate, and the soil is a xerochrept with a mean depth between 50 and 100 cm. The average precipitation is about 570 mm year^{-1}, and the mean annual temperature is 13 °C. During the period of study the mean precipitation was 518 mm year^{-1}, without significant differences (Wilcoxon ranks test) between the two sampling areas at the top and bottom of the valley (see *figure 1*). The forest is dominated by *Quercus ilex*, *Arbutus unedo* and *Phyllirea media*, followed by *Erica arborea*, *Acer monspessulanum*, *Sorbus aria* and *Ilex aquifolium* to a lesser degree [13]. A set of 69 plots (25 m^2 each plot) distributed at three alti-
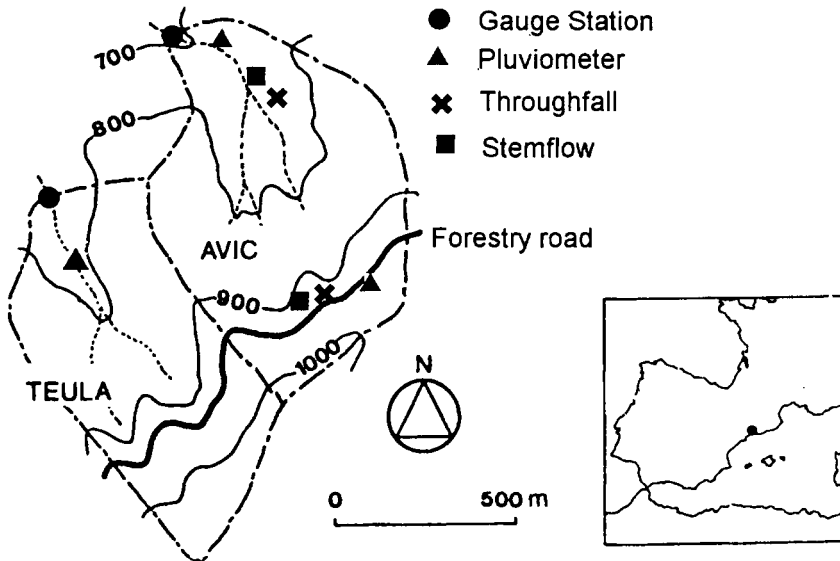

Figure 1. Location map for the Prades holm-oak forest and the Avic and Teula experimental catchments with reference to the sampling areas for rainfall pluviometers, THF and STF collectors and runoff gauge stations.

tudes (750, 850 and 950 m a.s.l.) across the Avic catchment showed a mean density of 9 178 stems ha^{-1} (ranging from 8 000 to 18 200 stems ha^{-1}), and a mean basal area of 37.9 m^2 ha^{-1} [29]. The calculated mean leaf area index (LAI) was 4.6 m^2 m^{-2} at the top and 5.3 m^2 m^{-2} at the valley bottom. Tree height ranged from 3 to 9 m [42]. Small differences were detected between the average catchment structure and the hydrology sample stand with only the three main species. The mean density of the last catchment structure was 8 460 stems ha^{-1}, with the LAI equal to 5.1 m^2 m^{-2} and 5-m high trees.

2.2. Methodology

To assess the hydrological flux in this forest, the following experimental design was used: ten rainfall collectors distributed in cleared areas at two different altitudes in the Avic catchment, at the top and at the bottom of the valley; one continuous rain gauge located at the valley bottom, 50 no-roving throughfall collectors, randomly located in a 950-m^2 forest plot at the top of the catchment, and four no-roving throughfall collectors located in the valley bottom forest plot; 20 stemflow collectors evenly covering the diameter rank distribution in the three major tree species (ten for *Q. ilex* in the top plot, five for *A. unedo* and five for *P. media* in the bottom plot). The location of the different gauges is shown in *figure 1*. The design used was planned to take into account the effect of the canopy multilayer structure, and to obtain global stemflow and throughfall values at the forest scale. Stemflow was sampled in small and large trees of the same canopy layer despite the fact that in the small trees it could be underestimated, unlike the isolated and uncovered trees. Throughfall and stemflow values obtained in this way could be more accurate for a canopy filter layer approach in a forest [6]. The sampling frequency was each rainfall event for throughfall and stemflow, and a continuous measurement for rainfall. The data series used in this work extended from June 1981 to November 1983.

Linear and power functions were fitted for each tree sampled to estimate the stemflow from precipitation as a function of tree size. Stemflow (STF) and throughfall (THF) at forest scale were processed, extending the average throughfall data from the sampling plot to the whole catchment surface and applying the stemflow equation from each tree sampled to the number of trees in the same diameter class in the reference area. Due to the resprouting structure of the Prades holm-

oak forest, the diameter was measured at 50 cm and called DKH (diameter at knee height). Interception (INT) was estimated by daily differences between precipitation (P) and STF plus THF.

The LAI was estimated using the relationship between the increment of light extinction and that of the leaf area index in the canopy profile [25]. In three square columns (0.5 × 0.5 m), the light extinction was measured with a sunfleck ceptometer (Delta T device) at every 0.5 m difference in height. Eleven readings for light extinction were obtained from each column located randomly in three areas in the canopy. Leaves were collected every 125 dm^3 (0.5 m deep), in the three 5-m tall columns. Samples were transported to the laboratory, and leaf area was measured with a leaf area meter Li-3000 (LiCor Inc.). An exponential regression between the mean LAI measurements and average light extinction was established and used to estimate the LAI from measurements of light extinction with the ceptometer located over each THF collector in the plot.

The projected crown area was estimated assuming a circular projection area (crown = πR^2) for each tree, where R was the mean distance between the tree trunks and the end of the branch projection. A linear correlation between mean stem diameter and projected crown (m^2) was established in a set of 72 *Q. ilex* trees classified in 11 DKH classes. The fitted function was: crown (m^2) = 1.017 + 1.064 * DKH (cm), with R^2 = 0.689 (d.f. = 9). Using this function, the projected crown area was calculated for each of the ten *Q. ilex* trees sampled for STF.

3. RESULTS AND DISCUSSION

3.1. Stemflow

3.1.1. Stemflow average and tree size influence

Table I shows the fitted functions (linear and power) between P and STF for each tree sampled in the three species. All regression equations were significant at 95 %, showing that intercepts and regression coefficients of the linear regression equations increase with DKH. A Student's *t*-test of significance of differences between pairs of regression coefficients in ascending order,

Table I. Linear and power regression adjusted with the daily data ($n = 39$) for STF (L) in three species (*Quercus ilex, Arbutus unedo* and *Phyllirea media*) and precipitation (P), for all sampled trees. DKH: diameter at knee height; SF: stemflow.

Species	DKH (cm)	Linear equation	R^2	Power equation	R^2
Quercus ilex	1.9	SF = − 0.217 + 0.024 * P	0.939	SF = 0.002 * P $^{1.442}$	0.975
	4.1	SF = − 0.944 + 0.072 * P	0.862	SF = 0.002 * P $^{1.674}$	0.929
	4.6	SF = − 1.015 + 0.106 * P	0.791	SF = 0.029 * P $^{1.250}$	0.787
	6.2	SF = − 0.349 + 0.430 * P	0.960	SF = 0.468 * P $^{0.978}$	0.960
	6.0	SF = 0.899 + 0.069 * P	0.650	SF = 0.381 * P $^{0.656}$	0.733
	11.7	SF = − 1.218 + 0.273 * P	0.922	SF = 0.211 * P $^{1.042}$	0.915
	12.6	SF = − 2.305 + 0.347 * P	0.912	SF = 0.187 * P $^{1.114}$	0.901
	15.1	SF = − 2.977 + 0.619 * P	0.938	SF = 0.356 * P $^{1.106}$	0.935
	19.1	SF = − 3.825 + 0.603 * P	0.922	SF = 0.278 * P $^{1.150}$	0.918
	23.4	SF = − 6.703 + 1.393 * P	0.929	SF = 0.809 * P $^{1.104}$	0.926
Arbutus unedo	2.8	SF = 0.060 + 0.096 * P	0.730	SF = 0.161 * P $^{0.888}$	0.738
	3.2	SF = − 0.318 + 0.072 * P	0.785	SF = 0.036 * P $^{1.140}$	0.787
	5.4	SF = − 1.480 + 0.234 * P	0.712	SF = 0.122 * P $^{1.122}$	0.707
	7.0	SF = − 1.603 + 0.625 * P	0.843	SF = 0.426 * P $^{1.076}$	0.844
	10.5	SF = 2.276 + 0.425 * P	0.776	SF = 0.780 * P $^{0.853}$	0.780
Phyllirea media	3.2	SF = − 0.958 + 0.087 * P	0.935	SF = 0.007 * P $^{1.489}$	0.975
	3.8	SF = − 1.393 + 0.175 * P	0.915	SF = 0.021 * P $^{1.435}$	0.957
	6.5	SF = − 0.324 + 0.428 * P	0.947	SF = 0.526 * P $^{0.951}$	0.948
	7.0	SF = − 1.643 + 0.239 * P	0.805	SF = 0.126 * P $^{1.118}$	0.796
	13.7	SF = − 1.477 + 0.361 * P	0.922	SF = 0.239 * P $^{1.033}$	0.916

using their standard error, showed that 80 % of regression coefficients increased significantly from one tree to another and with DKH [5]. Both types of function showed the effect of tree size, since the allometric relationship has a more structural sense. Further calculations of STF were made using the power function.

To calculate STF at the catchment level (under a spatially uniform rainfall hypothesis), the DKH distribution of the three species can be converted into the amount of water reaching the forest soil by applying their particular equations (*table I*). Total daily STF collected by all trees was calculated on a ground area basis. A general equation to estimate the daily STF from the amount of P in the Avic forest catchment was obtained. The fitted function was: STF (mm) = − 0.285 + 0.133 * P (mm); with R^2 = 0.995 and n = 60 (*figure 2*). At forest scale,

the results (*table II*) indicate that the total STF in the Avic catchment forest was 62 mm year^{-1}. In spite of being the dominant tree (71 % of the number of trees ha^{-1}), *Q. ilex* only contributes 55 % of the annual STF, *A. unedo* 32 % and *P. media* 13 %. The *A. unedo* species, probably because of its particular branch structure and crown shape, presents the highest STF values per tree.

The trunk diameter at 0.5 m high (DKH) was also incorporated into a multiple regression function to improve the performance of the model, since the DKH reflects the size of the tree crowns. Different equation types (linear, logarithmic and other equations from the literature) were applied to a data set of daily values. The highest correlation coefficient was obtained for all species with the logarithmic function (*table III*). Only in the case of *Q. ilex* was the R^2
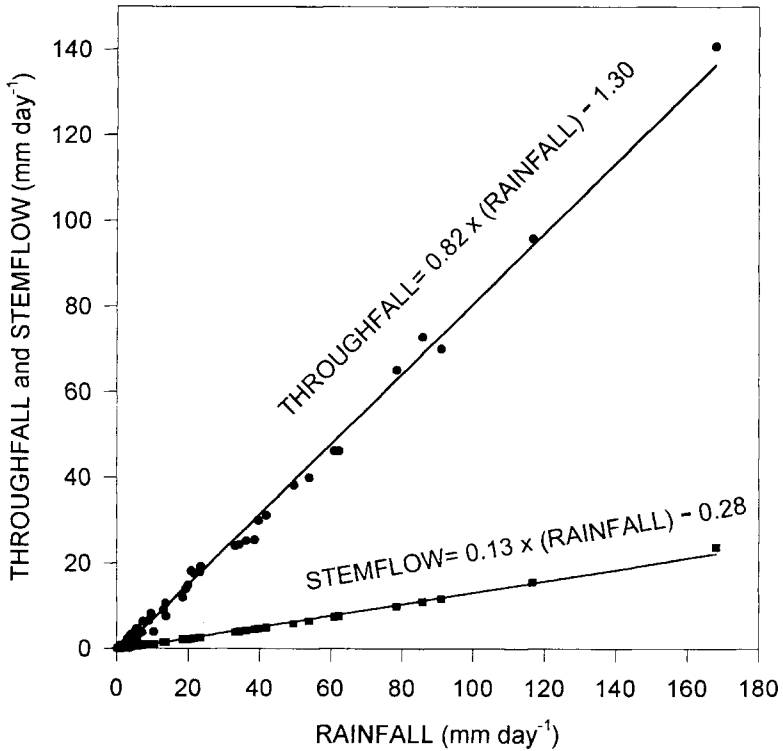
Figure 2. Relationship between daily precipitation and THF and STF volume at the catchment level in the Avic forest. Both linear fitted equations are significant (at $P < 0.001$). From the equations, the threshold to obtain valid values for THF and STF are 1.58 and 2.14 mm, respectively.

Table II. Distribution of species by diameter class and their contribution to the STF at forest scale in the Avic catchment. The percentage values refer in both cases (density and STF) to the global estimation in the Avic forest catchment. DKH: diameter at knee height.

DKH classes (cm)	Density (trees ha⁻¹)			Stemflow per diameter class (mm year⁻¹)		
	Q. ilex	A. unedo	P. media	Q. ilex	A. unedo	P. media
< 2.5	585	69	191	0.516	0.364	0.510
2.6–5.0	2220	516	522	4.858	1.658	3.328
5.1–7.5	1240	458	208	4.777	9.045	3.366
7.6–10.0	823	330	52	4.082	6.516	0.841
10.1–12.5	551	64	6	6.620	1.616	0.083
12.6–15.0	301	29	6	4.233	0.732	0.083
15.1–17.5	162	–	–	4.353	–	–
17.6–20.0	87	–	–	2.154	–	–
20.1–22.5	40	–	–	2.419	–	–
Σ	6009	1466	985	34.01	19.93	8.21
%	71.0	17.3	11.7	54.7	32.1	13.2

Table III. Multiple regression between precipitation amount (P in mm), tree diameter at knee height (D in cm) and STF (in L), for the three studied species. Model 1 was proposed by Haworth and McPherson [19] and Model 2 was used by Aussenac [3]. All models are significant at $P < 0.001$.

	Multiple regression functions	R^2	d.f.
Quercus ilex			
Linear	STF = – 0.0001 + 0.45 * P + 0.50 * D	0.383	369
Logarithmic	Ln (STF) = 0.0006 + P$^{1.664}$ + D$^{1.451}$	0.651	369
Model 1	Ln (STF) = 0.930 – 6.51* e$^{-0.056* P}$ + 0.161 * D	0.803	369
Model 2	Ln (STF) = –Ln 4.9 + 1.62* Ln P + 0.05* D^2	0.577	369
Arbutus unedo			
Linear	STF = – 12.344 + 0.29 * P + 2.09 * D	0.570	192
Logarithmic	Ln (STF) = 0.0014 + P$^{1.425}$ + D$^{1.941}$	0.818	192
Model 2	Ln (STF) = – Ln 4.7 + 1.59* Ln P + 0.025* D^2	0.750	201
Phyllirea media			
Linear	STF = – 5.790 + 0.258 * P + 0.678 * D	0.691	192
Logarithmic	Ln (STF) = 2.185 + P$^{1.509}$ + D$^{-2.52}$	0.859	192
Model 2	Ln (STF) = – Ln 3.9 + 0.74* Ln P^2 + 0.004* D^2	0.598	203

improved using the function proposed by Haworth and McPherson [19], which was applied also to a tree of the *Quercus* genus (*Q. emory*) with similar results. For the other species (*A. unedo* and *P. media*), this equation was not statistically significant, probably due to the different branch structure and tree shape.

3.1.2. Concentration ratio of stemflow to tree crown projection

The relationship of the STF values to the projected crown area or to the basal area reflects the capacity of different trees to concentrate rainfall water from the canopy layer to the area around their trunks. Aussenac [2], Falkengren-Grerup [15], Tanaka et al. [44] and others suggest that STF infiltration water could reach a distance no greater than 30 cm from the trunk. But Nàvar and Bryan [31], modifying the equation of Herwitz [21], proposed a model to relate the infiltration area around the tree trunks as a function of trunk basal area (B), stem diameter and distances covered by infiltration excess travel (D_r). The proposed model is $D_r =$

$\sqrt{(I + B/2) / (\pi/2)} - (d/2)$, where I is the infiltration area (m^2); B is trunk basal area (m^2); and d is trunk diameter (m). According to these authors, STF infiltrates in a circle or semi-circle whose average radial distances depend on rainfall intensity, soil infiltration capacity and slope angle, and rarely exceed 15 cm. In spite of these parameters being highly variable, the application of this model to the sampled trees provides an estimate of the surface area from 1.2 to 117 cm^2 (*table IV*) in an event of 85.7 mm rainfall, with a 960-min duration and a mean intensity of 8.2 mm h^{-1}.

The Herwitz approach [21] was used to calculate the crown contributing area, as well as the funnelling ratio for each of the ten sampled trees (*table V*). The funnelling ratio shows the highest values for the small trees, independently of their projected crown surfaces. As can be observed in *tables IV* and *V*, the calculated infiltration area is very small, based on a soil infiltration capacity of 820 mm h^{-1} (1.36 cm^3 cm^{-2} min^{-1}) recalculated from Piñol's [35] measurements using a ring infiltrometer (0.3 m diameter).

Table IV. Estimated input rates, infiltration area and overland flow distances of infiltration excess in the precipitation event of highest intensity. The infiltration area calculations are based on a soil infiltration capacity of 820 mm h^{-1} (1.36 cm^3 cm^{-2} min^{-1}).

Rainfall (mm)	Time (min)	Tree diameter (cm)	Stemflow (L)	Input rate (cm^2 min^{-1})	Infiltration area (cm^2)	Radial distance (cm)
85.7	960	1.9	1.62	1.68	1.23	0.3
		4.1	3.23	3.36	2.47	0.3
		4.6	7.88	8.20	6.03	0.7
		6.0	5.02	5.23	3.84	0.4
		6.2	43.22	45.02	33.10	2.4
		11.7	19.31	20.11	14.78	0.7
		12.6	26.85	27.97	20.56	1.0
		15.1	60.86	63.39	46.61	1.7
		19.1	52.67	54.86	40.34	1.2
		23.5	153.05	159.43	117.22	2.8

Only for the tallest tree does the calculated radial distance of infiltration excess approach 3 cm from the trunk. The high infiltration capacity of the Prades forest soil (820 mm h^{-1}) seems to be the main factor in reducing the distance of infiltration excess.

On an annual scale (*table V*), for 518 mm of mean P during the period of study, the measured STF volume for these trees ranged from 9 L year^{-1} in small trees to 605 L year^{-1} in large trees. These figures represent the amount of water received from a crown contributing surface ranging from 0.017 to 1.17 m^2, only infiltrated over an area of 0.0117 m^2 in the large sampled tree. These small areas receive high amounts of water in terms of mm equivalent to rainfall. Another way of comparing the STF concentration capacity with respect to rainfall is to take into account the proposed 15-cm trunk distance for STF infiltration. In this case, the surface area of distribution around the tree trunk represents on average 362 cm^2 (*table V*). On this assumption, the annual water received around the trunk of a medium tree of 12.6 cm DKH is equivalent to 3 874 mm annual precipitation. In open spaces the water received is 518 mm, while 389 mm is received as THF under canopy cover when the distance is more than 15 cm from the trunks. In summary, these areas

around the tree trunks receive less water by STF than THF for the smallest trees, but nearly 30 times the average THF for the large trees.

3.1.3. Stemflow in relation to the evapotranspiration needs of trees

In order to evaluate its relevance, STF can be compared with the tree evapotranspiration in this Mediterranean forest. The average annual evapotranspiration in the Avic forest catchment was calculated by water balance after 10 years of study as 458 mm [7, 36]. This quantity is distributed by crown surfaces, assuming that evapotranspiration is proportional to the respective tree basal areas. The mean annual tree evapotranspiration is estimated by distributing the annual water (458 mm) among the number of trees in each diameter class. As a result of this assumption, trees with 6.0 and 23.5 cm diameters would annually evaporate amounts of 551 and 1 136 L, respectively. Comparing these estimated values with the STF measured in the sampled trees (*table V*), we can observe that in the small trees (DKH = 6.0 cm) the stemflow measured was 49 L, and in the large trees (DKH = 23.5 cm), it reached 605 L

Table V. Size characteristics of the experimental canopy trees of *Quercus ilex*, their annual STF yield, the estimated overland flow, the funnelling ratio and the received water equivalent to rainfall.

Tree diameter (cm)	Calculated projected crown (m²)	Measured stemflow (L tree⁻¹)	Basal area (cm²)	Canopy contributing area (m²)	Funnelling ratio	Estimated infiltration area (cm²)	Water received equivalent (mm)	Enrichment factor over 518 mm
1.9	4.8	8.83	2.8	0.017	60.88	354	249.43	0.5
4.1	5.8	21.88	13.2	0.042	32.00	354	614.60	1.2
4.6	6.1	38.52	16.6	0.074	44.79	356	1 082.02	2.1
6.0	6.8	49.60	28.2	0.096	33.95	358	1 385.47	2.7
6.2	7.6	213.60	30.1	0.412	136.99	358	5 966.48	11.5
11.7	9.4	120.17	107.5	0.232	21.58	362	3 319.61	6.4
12.6	9.8	140.64	124.6	0.271	21.79	363	3 874.38	7.5
15.1	11.0	268.72	179.0	0.518	28.98	365	7 362.19	14.2
19.1	12.9	247.65	286.0	0.478	16.71	368	6 729.62	13.0
23.4	14.9	604.92	430.0	1.167	27.15	371	16 305.12	31.5

per year. These figures highlight the significance of STF, because on average this flow only corresponded to 39 % of the water transpired by the trees, ranging from 9 % in the small trees to 53 % in the large trees.

3.2. Throughfall

3.2.1. Throughfall average and spatial variability

In all forested soils, THF normally represents the major way in which soil water is recharged, and an average value is generally assumed in spite of the irregular distribution over the covered soil surface. The fact is that, as usual, the average THF value is the only reference to this flux in many areas. The amount of P is the main factor in determining the THF average value (*figure 2*), and there is a positive and significant ($R^2 = 0.995$, $n = 60$) linear correlation (THR $= 0.82 * P - 1.30$). However, the observed THF data from the 50 collectors used in the Prades forest reflect the spatial variability of the daily rainfall redistribu-

tion. *Figure 3* shows the relationship between P and THF, as well as the maximum and minimum values observed in each rain event. From this relationship, the variability can once again be appreciated: the asymmetric distribution of maximum and minimum values on either side of the mean. Across all ranges of P, some collectors take more water than average, and even exceed the P in open areas. On the contrary, other areas receive less water than the average. An explanation of these results may be the existence of preferential routes or dripping points in the canopy layer that concentrate the water from a part of the canopy. If this pattern were constant in time, soil moisture would be higher than average at these points, while others would be considered as dry soil sites in the same forest.

As the canopy depth is the main factor to intercept rainfall water in the canopy layer approach, a preliminary hypothesis could be the association of the THF amount at each soil point, with the LAI in the part of the canopy covering each collector. To examine this effect on spatial THF variability, a one-way variance analysis
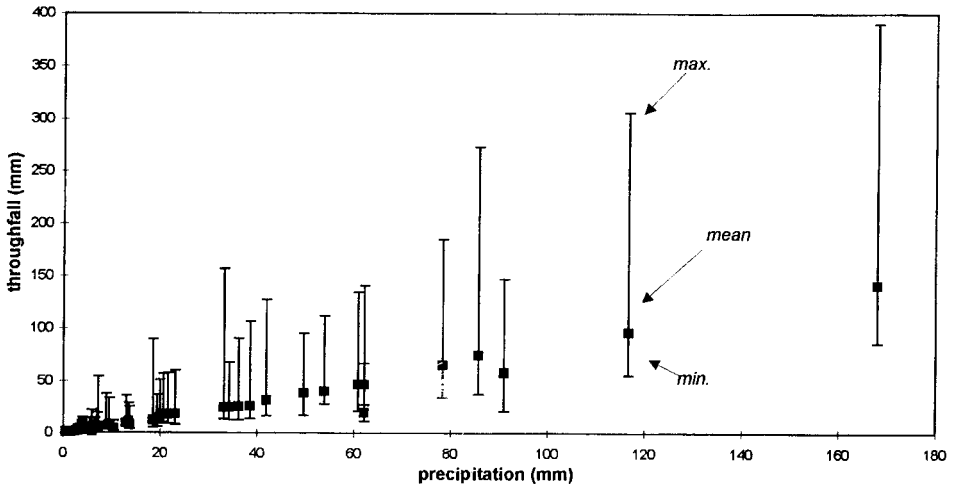

Figure 3. Daily THF (average, minimum and maximum) and precipitation relationship in a set of 50 collectors under the Mediterranean forest canopy of the Prades catchment.

(ANOVA) was performed. The four LAI values found over collectors were used to calculate the four THF average values in each LAI class (*table VI*). The results show that although lower amounts of THF correspond to high LAI values, these differences were not significant.

The spatial THF variability measured by the daily coefficient of variation (CV %) in the 50 collectors was higher for small storm events and decreased asymptotically as rainfall increased [5]. Furthermore, the frequency in distribution of collectors is modified according to the amount of rainfall. Small rainfall events present an inverse *J*-distribution of collectors (largely skewed to the right), because only a few collectors in favourable positions under dripping branches received more THF amounts than most of the others. In big rainfall events, collectors receive more uniform amounts of THF with more normal distribution results. The skewness statistical parameter was calculated for these distributions, and their values versus the rainfall amount and maximum intensity are presented in *figure 4*. All the skewness parameter values were greater than zero, showing a positive asymmetry, thereby confirming the deviation shown in *figure 3*. The highest values (5.01 and 4.65) were found for rainfall events of low intensity and volume, whilst the opposite was observed when these rainfall events had a high volume and were near the normal dis-

tributions. In this case, their skewness parameters were near zero.

3.2.3. Spatial independence of throughfall collectors

As has been indicated, THF collectors are normally distributed under the stand only in the heavy rainfall events, being largely skewed and temporally changing in the rest. The shapes of this distribution reveal any fixed structure of dripping points in the canopy layer. Following Loustau et al. [28], the spatial independence of THF individual collectors was checked using a variogram analysis (GEO-EAS software [12]). Each of the computed variograms had a horizontal linear shape, as shown in *figure 5*. The shape of the variograms did not reveal any structure of spatial auto-correlation between the measurements of THF. This means that the variance of THF did not show consistent variation as the distance between the two points of THF measurement increased. Therefore, the measurements of THF for each collector were assumed to be independent of each other.

3.3. Interception

The INT of rainfall represents the precipitation fraction re-evaporated from the water retained and stored in the canopy, wet leaves and branches. From a hydrological

Table VI. Average, maximum and minimum values of THF in mm by class of LAI in the canopy, and result of the ANOVA test applied to the differences between LAI groups. THF: throughfall; LAI: leaf area index.

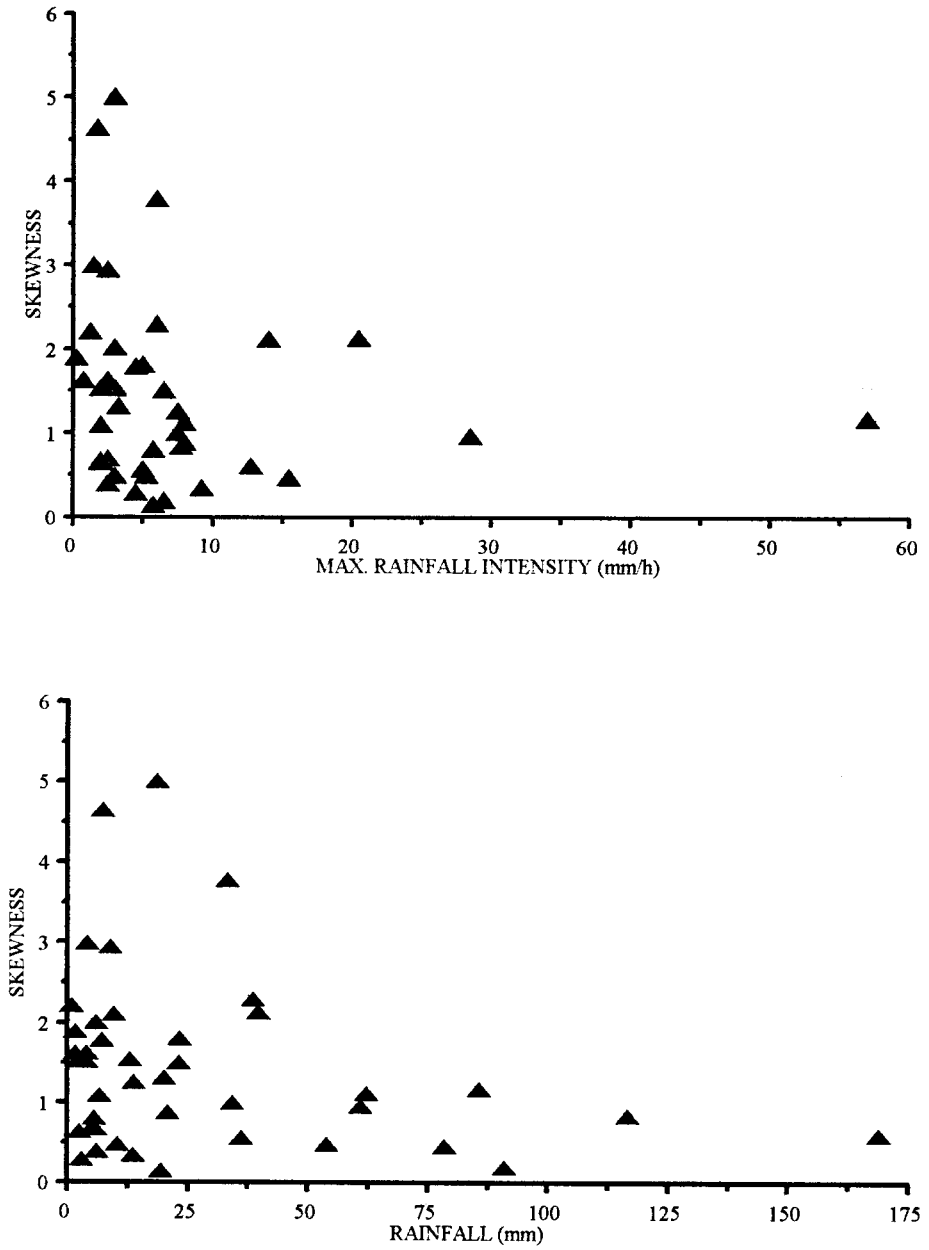| THF parameter	LAI class			
	0.5–1.9	2–2.9	3–3.9	4–4.9
Throughfall average	1 063.0	1 049	915.0	823.0
Maximum throughfall	1 212.5	1 788	1 361.5	1 142.5
Minimum throughfall	708.5	773	493.3	631
ANOVA by LAI	a	a	a	a

Figure 4. Skewness parameter for the daily THF collector distribution versus rainfall (lower graph) and maximum rainfall intensity (upper graph).
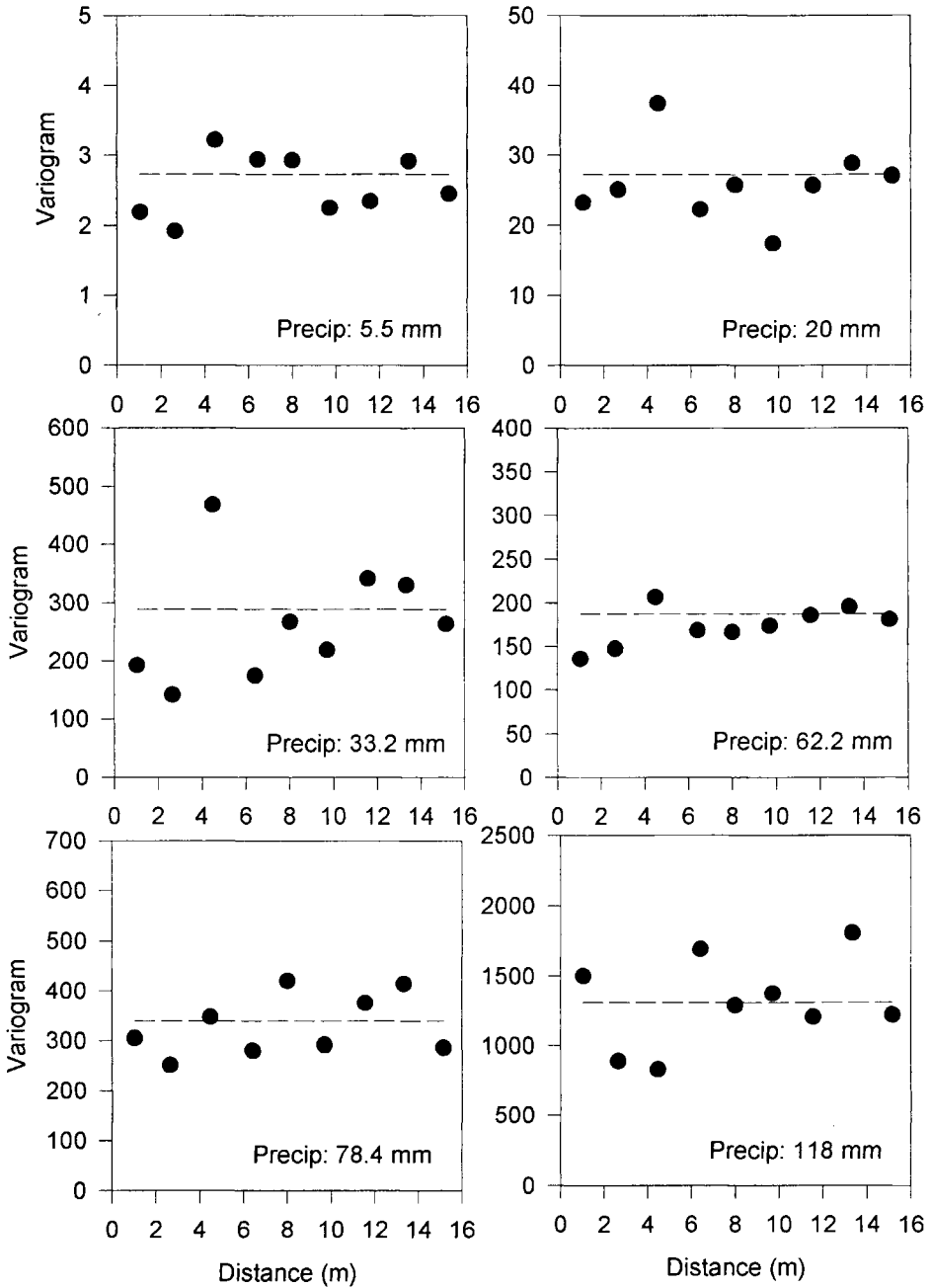
Figure 5. Global variograms of THF for six selected storms events covering a gradient of precipitation (from 5.5 to 118 mm). The total variance of THF is represented by the dashed horizontal line in each graph.

point of view, INT represents a fraction of the rainfall not reaching the forest soil. It is a loss of water in the sense of transpiration water, but it is not completely lost in the sense of the forest hydrological cycle because transpiration is reduced during the evaporation processes of the intercepted water on leaves [4, 40]. In common with the THF spatial pattern, INT also shows spatial variations within the forest resulting from differences in the canopy structure and variations in climatic conditions during and after rainfalls. Data from spatial dripping points in the Prades forest fully support these ideas on INT variability. The mean daily INT calculated as the difference between P less THF plus STF reflects the fact that daily INT is not constant, and shows a low variability decreasing with the rainfall. The relationship between INT and P (both in mm)

follows a significant ($R^2 = 0.561$ for $n = 60$) power expression (INT = $0.86 * P^{0.406}$), levelling off as the saturation capacity is reached.

The storage or saturation capacity as can be deduced from the power relationship seems to have a maximum value, with a magnitude that could be a function of both tree canopy structure and P characteristics during the event. The fitted curve equation in percentage form (*figure 6*) reflects a minimum levelling-off value near 10–12 % of the rainfall, with the highest percentage for the smallest rainfall events. In any case, the INT of rainfall by the forest canopy could be established between a minimum value equal to the sum of the thresholds for THF and STF (1.6 and 2.2 mm, respectively), and a maximum value near 10–15 mm in the gross rainfalls.
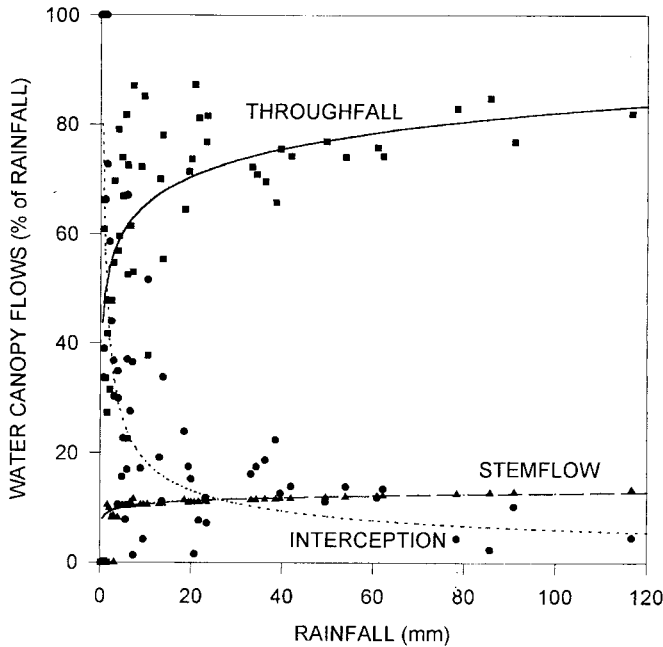

Figure 6. Daily data of the canopy water flows, THF, STF and INT (in percentage of rainfall), and their regression curves with gross precipitation (mm). The fitted equations are the following: THF = $28.84 + 13.82 * \text{Ln (P)}$, with $R^2 = 0.671$ and $n = 60$; STF = $3.41 + 2.46 * \text{Ln (P)}$, with $R^2 = 0.763$ and $n = 60$; and INT = $57.04 * (P)^{-0.49}$, with $R^2 = 0.608$ and $n = 60$.

3.4. Rainfall water redistribution at forest scale

The mean annual values of THF, STF and INT for the Avic holm-oak forest and their percentages of annual rainfall are presented in *table VII*. The importance of the STF (12.1 % of the total rainfall) is noticeable, as well as its similarity to the intercepted part of the rain (12.9 %). Throughfall is obviously the major pathway of rainfall water through the canopy layer (75 % of the total). There is a difference between the Avic forest data and that in the literature reviewed, which reports STF normally ranging from 1–5 % of rainfall [14, 23, 33]. *Figure 6* shows the fitted equations to the three water pathways in percentage of rainfall for the Avic holm-oak canopy. The fitted equations are significant ($P < 0.001$), and show the characteristic trend for each pathway. Throughfall and STF increase with rainfall amount, and INT decreases as rainfall increases.

To test which other factors of rainfall events besides the amount of the water influence the water pathways in the canopy, the correlation coefficient between THF, STF and INT and some parameters of rainfall events (maximum and average rainfall intensity, storm duration and previous dry period) were calculated. *Table VIII* shows the calculated correlation coefficients and demonstrates the positive effect of some of these parameters that can homogenize the differential effect of the canopy structure. Maximum intensity, rainfall duration and the relative duration of rainfall with an intensity higher than the average showed significant correlation coefficients with the three pathways. In contrast, mean intensity and dry period length previous to P did not have significant correlation coefficients with any water flow.

Table VII. Rainfall partitioning in the forest canopy at the Avic catchment.

Water flux	Study period (mm)	Annual water (mm/yr)	Rainfall (%)
Precipitation	1 296.26	518.50	100.00
Throughfall	972.37	388.94	75.00
Stemflow, three species	156.53	62.61	12.10
Q. ilex	85.53	34.21	54.7
A. unedo	49.83	19.93	31.9
P. media	20.21	8.21	13.4
Interception	167.36	66.94	12.90

Table VIII. Correlation coefficients (R) between some precipitation parameters and THF, STF and INT volume (mm), in the canopy of the holm-oak forest (* significant at $P < 0.01$). INT: interception.

Water flux	Mean intensity	Maxim. intensity	Rainfall time duration	Rainfall time > × intensity	Previous dry period	No. of events
Throughfall	0.029	0.567*	0.915*	0.889*	–0.043	38
Stemflow	0.069	0.472*	0.906*	0.876*	–0.063	34
Interception	–0.161	–	0.638*	0.681*	0.226	40

3.5. Effect of amount of precipitation on water pathway percentage

To explore the possible effect of the amount of P on the high stemflow values observed, P events were classified according to the amounts of rainfall. Seven rainfall classes (from less than 5 mm to more than 100 mm/event) allowed THF, STF and INT to be estimated within each rainfall interval. The results (*table IX*) show that, in the Prades forest, only 17 % of rainfall water is produced by small events (less than 20 mm), 21 % is produced by events between 20 and 40 mm, and the most noticeable fact is that 62 % of water comes in events with more than 40 mm. This particular rainfall event distribution is characteristic of the Spanish Mediterranean area [34], and is probably different from that of the temperate areas where the highest P frequency is less than 20 mm/event.

At catchment scale, THF, STF and INT have been calculated by regressions from gross rainfall for each of the seven classes (*table X*). Stemflow and THF change from 5 and 42 % when rainfall events are small (5 mm or less) to 14 and 83 %, respectively, for events with more than 65 mm, reducing the INT to 3 %.

As the amount of P is the major factor determining the spatial distribution of rainfall water on forest soils, the possible effect of a climatic change suggested by Rambal and Debussche [39] for the Mediterranean region was analyzed. These authors indicate that one of the possible effects of climatic changes is the increase in high daily rainfall class frequency (in particular rainfall higher than 25.6 mm day^{-1}), and the decrease in frequency of small events (less than 6.5 mm day^{-1}), whilst the annual rainfall and their monthly distribution do not seem to change significantly. Applying the Rambal and Debussche [39] prediction and assuming that the present behaviour is maintained, in the Prades forest the INT could be reduced to 5 % rainfall and STF and THF increased to 13 and 82 %, respectively (*table X*).

These changes can affect the rainfall water redistribution in the Mediterranean forest, with effects on the overland runoff water yield as a consequence of the STF increase and the infiltration effect [17]. It is assumed that for an area located in the transition zone between temperate and dry Mediterranean climates, these possible changes in rainfall water redistribution by the canopy can be relevant to water use by plants, and to the control of overland flow and soil erosion [11].

Table IX. Distribution of Prades rainfall events in all studied periods by precipitation class and percentage of received water volume by class.

Precipitation class (mm)	No. of events (n)	Water received (mm)	No. of events (%)	Water received (%)
0–5	25	45.59	41.66	3.51
5.1–10	9	62.81	15.00	4.84
10.1–20	7	108.65	11.66	8.38
20.1–40	9	270.94	15.00	20.90
40.1–65	5	268.47	8.33	20.71
65.1–100	3	255.10	5.00	19.67
100.1–200	2	284.70	3.33	21.96
200.1 <	0	0	–	–

Table X. Precipitation water redistribution by the major canopy tree species of the Avic forest canopy: throughfall (THF), stemflow (STF) and interception (INT). Annual values are given by precipitation classes, in mm and percentage of precipitation.

Precipitation class	Precipitation (mm year⁻¹)	Throughfall (mm year⁻¹)	Stemflow (mm year⁻¹)				Precipitation (%)		
			Quercus ilex	Arbutus unedo	Phyllirea media	All species	THR	STF	INT
0–5	18.23	7.64	0.52	0.30	0.09	0.91	41.94	5.04	53.02
5.1–10	25.12	16.81	1.15	0.69	0.23	2.07	66.90	8.26	24.84
10.1–20	43.46	28.72	2.12	1.31	0.45	3.88	66.08	8.96	24.96
20.1–40	108.37	80.67	6.71	4.09	1.53	12.33	74.44	11.39	14.17
40.1–65	107.39	80.66	7.05	4.19	1.69	12.93	75.11	12.05	12.84
65.1–100	102.04	83.71	7.13	4.10	1.76	12.99	82.03	12.74	5.23
> 100	113.88	94.62	8.71	4.74	2.24	15.69	83.09	13.79	3.12

REFERENCES

[1] Aussenac G., Interception des précipitations par le couvert forestier, Ann. Sci. For. 25 (1968) 135–156.

[2] Aussenac G., Action du couvert forestier sur la distribution au sol des précipitations, Ann. Sci. For. 27 (1970) 383–399.

[3] Aussenac G., Couverts forestiers et facteurs du climat : leur interactions, conséquences écophysiologiques chez quelques résineux, thèse, Université de Nancy, 1975.

[4] Aussenac G., L'interception des précipitations par les peuplements forestiers,La Houille Blanche 7/8 (1981) 531–536.

[5] Bellot J., Análisis de los flujos de deposición global, trascolación, escorentía cortical y deposición seca en el encinar de l'Avic (Sierra de Prades), Ph.D. thesis, Dept. Ecology, Univ. Alicante, 1989.

[6] Bellot J., Escarré A., Efecto del estado de desarrollo del bosque mediterráneo sobre la distribución del agua de lluvia y nutrientes en el suelo forestal, Opt. Med., Ser. Semin. 3 (1989) 221–225.

[7] Bellot J., Lledó M.J., Piñol J., Escarre A., Hydrochemical budgets, nutrient cycles and hydrochemical responses in the *Quercus ilex* forest of Prades catchments, in: Teller A., Mathy P., Jeffers J.N.R. (Eds.), Responses of Forest Ecosystems to Environmental Changes: Commission of the European Communities, Elsevier Appl. Sci., 1992, pp. 389–396.

[8] Beven K., Germann P., Macropores and water flow in soils, Water Resour. Res. 18 (1982) 1311–1325.

[9] Bolin B., Doos B.R., Jager J., Warrick R.A. (Eds.), The Greenhouse Effect, Climatic Change and Ecosystems, SCOPE 29, Wiley, Chichester, 1986, pp. 544.

[10] Chiew F.H.S., Whetton P.H., McMahon T.A., Pittock A.B., Simulation of the impacts of climate change on runoff and soil moisture in Australian catchments, J. Hydrol. 167 (1995) 121–147.

[11] Crabtree R.W., Trudgill S.T., Hillslope hydrology and stream responses on a wooded, permeable bedrock: the role of stemflow. J. Hydrol. 80 (1985) 161–178.

[12] Englund D., Sparks A., GEO-EAS (Geostatistical Environmental Assessment Software): User's Guide, Environ. Monitoring Systems Lab., U.S. Environ. Prot. Agency, 1988.

[13] Escarré A., Lledó M.J., Bellot J., Martin J., Esclapés A., Seva E., Rovira A., Sánchez J.R., Balance hídrico, meteorización y erosión, en una pequeña cuenca del encinar mediterráneo, Monogr. Icona 47 (1986) 57–115.

[14] Ettehad R., Lossaint P., Rapp M., Recherches sur la dynamique et le bilan de l'eau des sols de deux écosystèmes méditerranéens á chêne vert. Écologie du sol. Recherche coopérative sur programme N° 40, CNRS, Paris, 3 (1973) 198–288.

[15] Falkengren-Grerup U., Effect of stemflow on beech forest soils and vegetation in southern Sweden, J. Appl. Ecol. 26 (1989) 341–352.

[16] Ford E.D., Deans J.D., The effects of canopy structure on stemflow, throughfall and interception loss in a young Sitka spruce plantation, J. Appl. Ecol. 15 (1978) 905–917.

[17] Gonzalez-Hidalgo J.C., Bellot J., Soil moisture changes under shrub plant cover (*Rosmarinus officinalis*) and cleared shrub as response to precipitation in a semi-arid environment: stemflow effects, Arid Soil Res. Rehabil. 11 (1997) 187–199.

[18] Hanchi A., Rapp M., Stemflow determination in forest stands, For. Ecol. Manage. 97 (1997) 231–235.

[19] Haworth K., McPherson G.R., Effects of *Quercus emoryi* trees on precipitation distribution and microclimate in a semi-arid savana, J. Arid Environ. 31 (1995) 153–170.

[20] Helvey J.D., Patric J.H., Canopy and litter interception of rainfall by hardwoods in the Eastern United States, Water Resour. Res. 1 (1965) 193–206.

[21] Herwitz S.R., Infiltration excess caused by stemflow in a cyclone-prone tropical rainforest, Earth Surface Processes Landforms 11 (1986) 401–412.

[22] Jackson I.J., Relationships between rainfall parameters and interception by tropical forest, J. Hydrol. 24 (1975) 215–238.

[23] Johnson D.W., Lindberg S.E. (Eds.), Atmospheric Deposition and Forest Nutrient Cycling, Ecological Studies 91, Springer Verlag, New York, 1992.

[24] Kimmins J.P., Some statistical aspects of sampling throughfall precipitation in nutrient cycling studies in British Columbian coastal forest, Ecology 54 (1973) 1008–1019.

[25] Lang A.R.G., Xiang-Yuequin, Estimation of leaf area index from transmission of direct sunlight in discontinuous canopies, Agric. For. Meteorol. 37 (1986) 229–243.

[26] Loaciga H.A., Valdes J.B., Vogel R., Garvey J., Schwarz H., Global warming and the hydrologic cycle, J. Hydrol. 174 (1996) 83–127.

[27] Loshali D.C., Singh R.P., Partitioning of rainfall by three central Himalayan forests, For. Ecol. Manage. 53 (1992) 99–105.

[28] Loustau D., Granier A., Moussa F.H., Interception loss, throughfall and stemflow in a maritime pine stand. I. Variability of throughfall and stemflow

beneath the pine canopy. J. Hydrol. 134 (1992) 449–467.

[29] Lledó M.J., Compartimentos y flujos biogeoquímicos en una cuenca de encinar de Monte Poblet, Ph.D. thesis, Univ. Alicante, 1990.

[30] Mauchamp A., Janeau J.L., Water funnelling by the crown of *Flourensia cernua* and chihuahua desert shrubs. J. Arid Environ. 25 (1993) 299–306.

[31] Nàvar J., Bryan R., Interception loss and rainfall redistribution by three semi-arid growing shrubs in northeastern Mexico, J. Hydrol. 115 (1990) 51–63.

[32] Neal C., Robson A.J., Bhardway C.L., Conway T., Jeffery H.A., Neal G.P., Ryland G.P., Smith C.J., Walls J., Relationships between precipitation, stemflow and throughfall for a lowland beech plantation, Black Wood, Hampshire, southern England: findings on interception at a forest edge and the effect of storm damage, J. Hydrol. 146 (1993) 221–233.

[33] Nizinski J., Saugier B., Dynamique de l'eau dans une chênaie (*Quercus petraea* (Matt.) Liebl.) en forêt de Fontainebleau, Ann. Sci. For. 46 (1989) 173–186.

[34] Perez Cuevas A.J., (Coord.), Atlas climático de la Comunidad Valenciana, COPUT, Generalitat Valenciana, Colecció Territori No. 4, 1994, pp. 208.

[35] Piñol J., Hidrologia i biogeoquímica de conques forestades de les Muntanyes de Prades, Ph.D. thesis, Univ. Barcelona, 1990.

[36] Piñol J., Lledó M.J., Escarré A., Hydrological balance of two Mediterranean forested catchments (Prades, northeast Spain), Hydrol. Sci. J. 36 (1991) 95–107.

[37] Ponce V.M., Shetty A.V., A conceptual model of catchment water balance: 1. Formulation and calibration, J. Hydrol. 173 (1995) 27–40.

[38] Prebble R.E., Stirk G.B., Throughfall and stemflow on silverleaf ironbark (*Eucalyptus melanopholia*) trees, Aust. J. Ecol. 5 (1980) 419–427.

[39] Rambal S., Debussche S., Water balance of Mediterranean ecosystems under a changing climate, in: Moreno J.M., Oechel W.C. (Eds.), Global Change and Mediterranean-Type Ecosystems, Springer Verlag, New York, 1995, pp. 386–407.

[40] Roberts J., Pymar C.F., Wallace J.S., Pitman R.M., Seasonal changes in leaf area, stomatal and canopy conductances and transpiration from bracken below a forest canopy, J. Appl. Ecol. 17 (1980) 409–422.

[41] Rutter A.J., Morton A.J., Robins P.C., A predictive model of rainfall interception in forest. II: Generalization of the model and comparison with observations in some coniferous and hardwood stands, J. Ecol. 51 (1975) 191–203.

[42] Sabaté S., Canopy structure and nutrient content in a *Quercus ilex* L. forest of the Prades mountains: effects of natural and experimental manipulation of growth conditions, Ph.D. thesis, Univ. Barcelona, 1993.

[43] Scatena F.N., Watershed scale rainfall interception on two forested watersheds in the Luquillo Mountains of Puerto Rico, J. Hydrol. 113 (1990) 89–102.

[44] Tanaka T., Tsujimura M., Taniguchi M., Infiltration area of stemflow-induced water, Annu. Rep. Inst. Geosci., No. 17, Univ. Tsukuba, Institute of Geoscience, Japan, 1990.